Journal of Materials Processing Technology 219 (2015) 271–277

Contents lists available at ScienceDirect

Journal of Materials Processing Technology

journal homepage: www.elsevier.com/locate/jmatprotec

Effect of tool shoulder features on defects and tensile properties of friction stir welded aluminum 6061-T6

Luis Trueba Jr.[a,*], Georgina Heredia[b], Daniel Rybicki[c], Lucie B. Johannes[c]

[a] University of Texas of the Permian Basin, Mechanical Engineering, 4901 East University, Odessa, TX 79762, USA
[b] The University of Texas at El Paso, Department of Metallurgical and Materials Engineering, 500 West University Avenue, El Paso, TX 79968, USA
[c] NASA Johnson Space Center, Materials and Processes Branch, Houston, TX 77058, USA

ARTICLE INFO

Article history:
Received 2 July 2014
Received in revised form
22 December 2014
Accepted 24 December 2014
Available online 6 January 2015

Keywords:
Friction stir welding
Aluminum alloy 6061-T6
Surface quality
Weld strength
Defect formation
Additive-manufactured tooling

ABSTRACT

Six unique tool shoulder designs were produced with the objective of improved metal constraint and flow to the pin. The six tools were made of Ti–6Al–4V by metallic additive manufacturing. Each tool was used to produce butt welds using aluminum 6061-T6 plates. The welds were subjected to nondestructive evaluation and tensile testing to determine weld soundness and strength. A FSW tool shoulder having a raised spiral design produced the weld with the best combination of surface quality and mechanical properties. The additive-manufactured Ti–6Al–4V tooling had good wear characteristics and appears to be a suitable route to rapidly produce unique FSW tool designs.

1. Introduction

A common defect that occurs with friction stir welding (FSW) is cavity formation near the weld centerline, adversely affecting the weld's mechanical properties. These weld defects are related to poor metal flow and constraint. In this paper, we explore the role of FSW tool shoulder features on metal flow, defect formation, and mechanical properties in aluminum 6061-T6 FSW butt joints.

Friction stir welding (see Fig. 1) is a solid state welding process in which a rotating tool comprising a shoulder and a pin is plunged into the metal being welded. The shoulder either applies a predetermined amount of force to the weld metal (load control) or is plunged a specific distance into the top surface of the metal (displacement control). The rotating tool is then moved along the joint line of the pieces being welded. Frictional heat supplied by the tool rotation plasticizes the metal allowing it to flow under the influence of the shoulder and pin. Under the normal force applied by the tool shoulder, the frictional and deformational heat assist in the bonding of the plasticized metal, allowing the weld to be completed behind the pin. The process parameters affecting the final weld properties include plunge force (or plunge depth), rotational speed, weld speed, tool tilt angle, and tool geometry.

Material flow in friction stir welds is complex; however, an understanding of the metal flow is essential to proper tool design in order to minimize the occurrence of defects. As shown in Fig. 2, metal flows around the pin in the direction of tool rotation while at the same time flowing upward near the pin before being redirected down by the shoulder toward the outside of the weld. The upward movement of the metal is caused by the metal displacement as the pin moves through the joint combined with the constraining action of the shoulder and backing plate. The rotation of the tool during the weld results in displacement of metal from the advancing side to the retreating side of the weld and a corresponding microstructural asymmetry. In addition, there is asymmetry between the root and crown of the weld due to the rotating shoulder being present only at the top of the weld. The quality of welds produced in FSW is dependent on this complex material flow and on the ability of metal to fill-in and mix behind the pin as it moves through the weld. If there is an insufficient quantity of metal rejoining and mixing behind the pin, defects such as porosity and insufficient bonding may occur. The resulting FSW microstructure is clearly a direct result of material flow during the welding process.

Mandal (2002) and Mishra and Mahoney (2007) have compiled and discussed common imperfections found in friction stir welds. Imperfections observable by visual inspection include galling,

* Corresponding author. Tel.: +1 432 552 3218; fax: +1 432 552 2433.
E-mail addresses: trueba_l@utpb.edu, luis.trueba@me.com (L. Trueba Jr.).

http://dx.doi.org/10.1016/j.jmatprotec.2014.12.027
0924-0136/

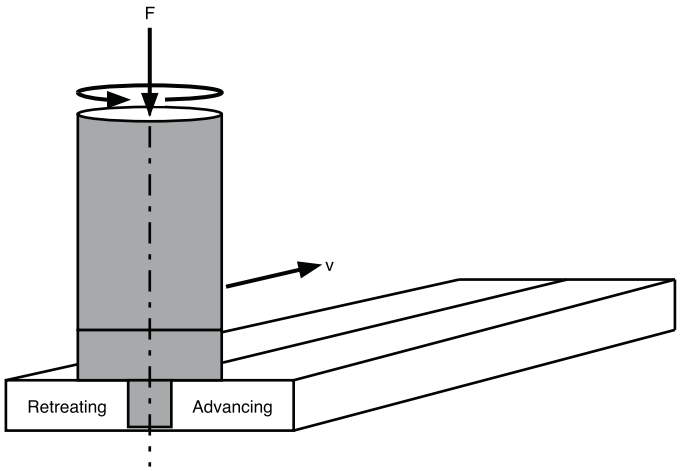

Fig. 1. Schematic representation of the friction stir welding process showing advancing and retreating sides of the weld.

excessive flash formation, smearing, and incomplete welds. Galling is caused by tool wear or excessively hot processing conditions in which weld metal adheres to the shoulder and is not re-deposited back into the weld giving the appearance of a rough weld surface. Flash formation occurs under excessive tool plunge force or displacement, while smearing is caused by insufficient contact of the shoulder along the top surfaces of the metal to be joined. Microscopic defects include voids, joint line remnants, and incomplete root penetration. Many of these defects can be revealed through metallographic examination of the weld joint. Cavities and incomplete root penetration can be revealed through X-ray radiography.

A review of tool designs by Mishra and Mahoney (2007) revealed that early tool designs used simple tool geometries comprising a cylindrical, threaded, fixed pin with a concave shoulder machined from tool steel. The concave shoulder of these tools constrains material that is displaced by the pin and acts as a metal reservoir. As the tool advances, the newly deformed metal is pushed into the shoulder cavity where it is then directed back toward the pin. Since then, tools have been developed with more sophisticated geometries that permit welding of thicker sections and improve weld quality.

It is possible to improve metal flow and frictional heating by employing various shoulder features. Mishra and Mahoney (2007) reported that early attempts by The Welding Institute to use a tool with convex shoulder features were unsuccessful because the convex shape pushed material away from the center of the tool. Since that time, raised and recessed shoulder features have successfully been used. These features include scrolls, ridges, grooves and concentric circles. While studying the effect of shoulder geometry on weld properties, Scialpi et al. (2007) found that a simple shoulder design with a concave shoulder feature and filleted edge produced better welds in terms of strength and surface quality compared to a tool having a recessed shoulder scroll and an edge fillet. Scrolled shoulder features direct deformed material toward the center where the pin is located, and eliminate the need for a tilt angle as well as excessive flash formation. With regard to shoulder diameter, Elangovan and Balasubramanian (2008) found that a shoulder-to-pin-diameter ratio (D/d) of three gave optimum mechanical properties irrespective of pin design. While there have been many studies published in the literature detailing successful overall tool geometries and pin features, there are few studies of the effect of tool shoulder features on metal flow and defect formation. Therefore, the objective of this study was to evaluate FSW tools with unique shoulder features specifically designed to improve the flow of metal toward the central pin during weld formation.

2. Experimental procedure

Six unique shoulder designs were produced for this experiment. An overall schematic of the tool design is given in Fig. 3; the individual shoulder designs are presented in Fig. 4. All tools were designed to rotate in a counterclockwise direction, and each tool was fitted with a non-threaded, flat-bottom, cylindrical pin. Each tool with the exception of tool F incorporated either a raised or recessed "fan" design to facilitate flow of metal toward the pin. Design F incorporated a ramp feature with a surface that increased in height opposite the direction of rotation and in the direction of the pin. The raised features were 0.5 mm above the shoulder height, and the recessed features were 0.5 mm below the shoulder height. A wiper feature was included around the outer diameter of the shoulder of tool A to evaluate the effectiveness of a wiper to improve the surface finish of welds.

The tools used in this study were manufactured by electron beam melting (EBM) on an Arcam A2 additive manufacturing machine. This allowed the complex tool geometries to be produced in a relatively short amount of time. The tools were manufactured of Ti–6Al–4V; yield and tensile strengths of this material have been reported by Rafi et al. (2013) to be 869 MPa and 928 MPa, respectively. The AISI 1090 steel pins were press-fit into the tools.

Plates of aluminum 6061-T6 with dimensions 15.24 cm × 10.16 cm × 0.635 cm were welded in the butt-configuration. The nominal composition of aluminum 6061 is 1.0% Mg, 0.6% Si, 0.30% Cu, 0.20% Cr. In preparation for welding,

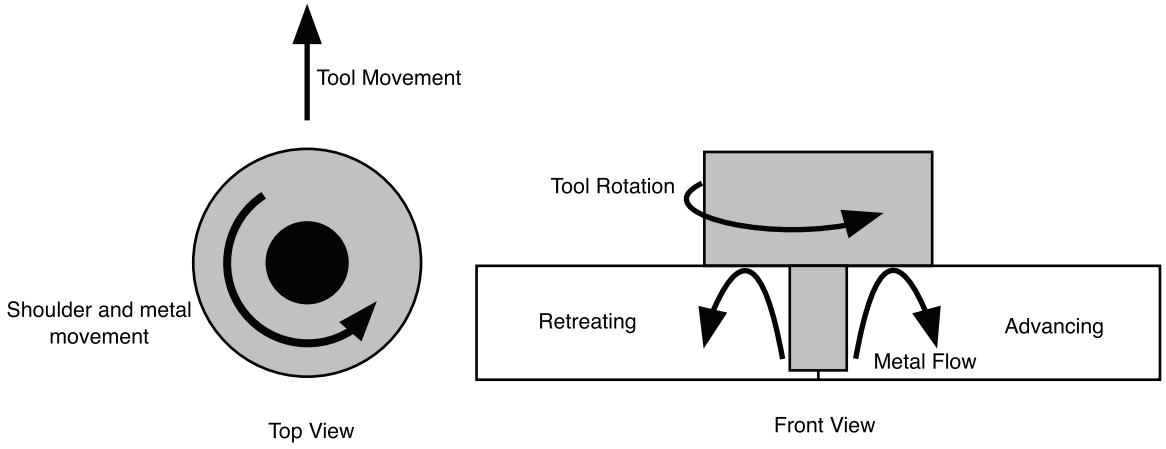

Fig. 2. Schematic showing direction of metal flow under rotating FSW tool shoulder.

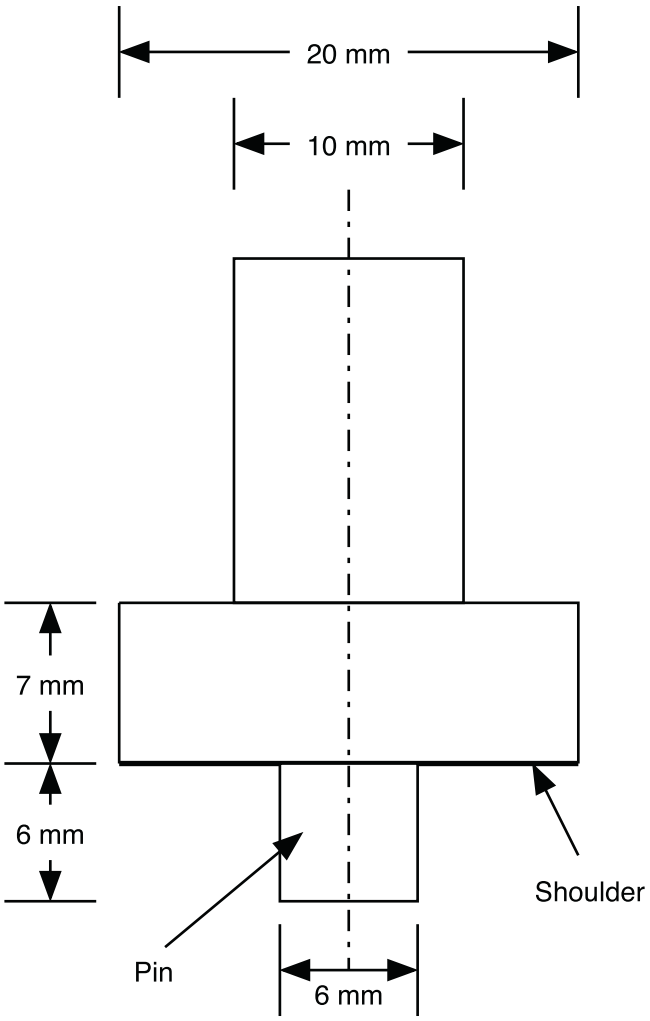

Fig. 3. Schematic diagram showing the major dimensions of the friction stir welding tools used.

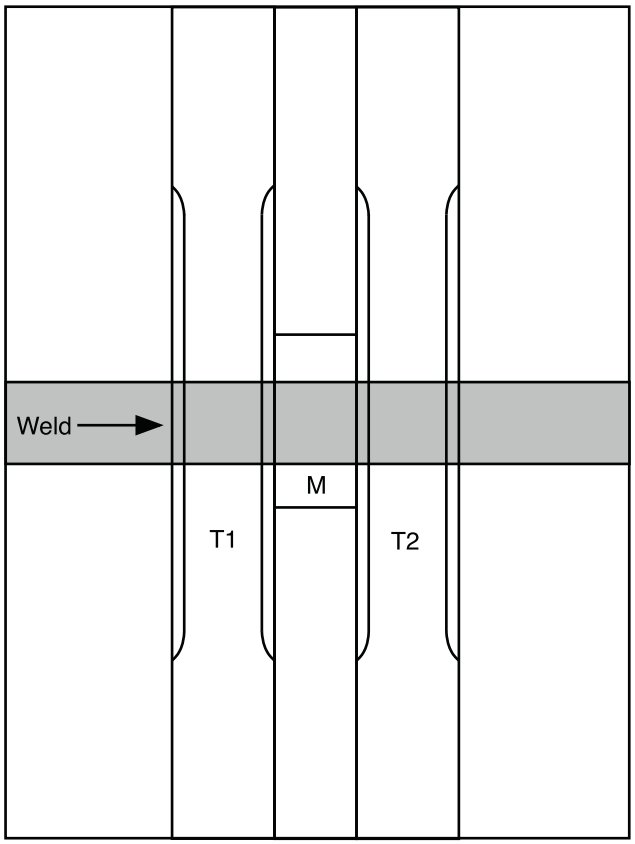

Fig. 5. Schematic diagram of welds showing sample locations. Samples T1 and T2 were used for tensile testing while sample M was used for metallography and microhardness measurement.

the faying surfaces of the plates were cleaned with alcohol. The welds were all produced parallel to the rolling direction using a plunge depth of 0.254 mm (measured from the raised surfaces of the tool) with a rotational speed of 1200 rpm and linear tool speed of 8.10 cm/min. The entrance of the tool into the joint was performed in the direction of the weld rather than by plunging in a direction normal to the weld seam.

After completion of the welds, the quality of each weld was evaluated through visual examination and X-ray radiography. The welds were then sectioned as indicated in Fig. 5 to produce samples for tensile testing and metallography. Two samples from each weld were used to determine its yield strength, tensile strength, and ductility. The reduced sections of the tensile samples were 102 mm long, 19 mm wide and 6.35 mm thick with a gage length of 50.8 mm. Short transverse metallographic samples were prepared from the center portions of the welds using standard metallographic procedures. Lastly, microhardness measurements (Vickers, 500 g load) were taken using the metallographic samples at three-mm intervals along lines traversing the top, center and bottom of each metallographic weld sample.

3. Results

3.1. Visual inspection

The weld crowns produced in this study are shown in Fig. 6. Varying amounts of flash formation were observed on the retreating side of all weld samples while minimal flash was observed on the advancing side. In addition, all of the samples exhibited excessive gathered flash on the advancing side at the weld exit. Due to the nature of the tool introduction and exit, keyholes were present at the entrances and exits of the welds. Metal was visible in the bottom of the exit keyholes for all welds except weld C. In addition,

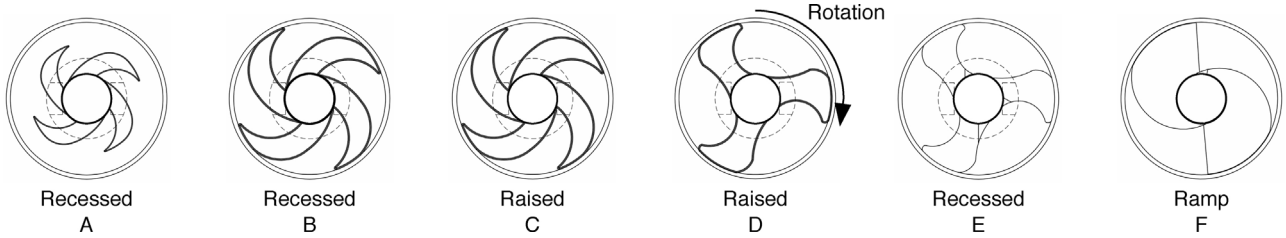

Fig. 4. Schematic diagrams of shoulder designs used. All tools were designed for counter clockwise rotation (clockwise in this bottom view).

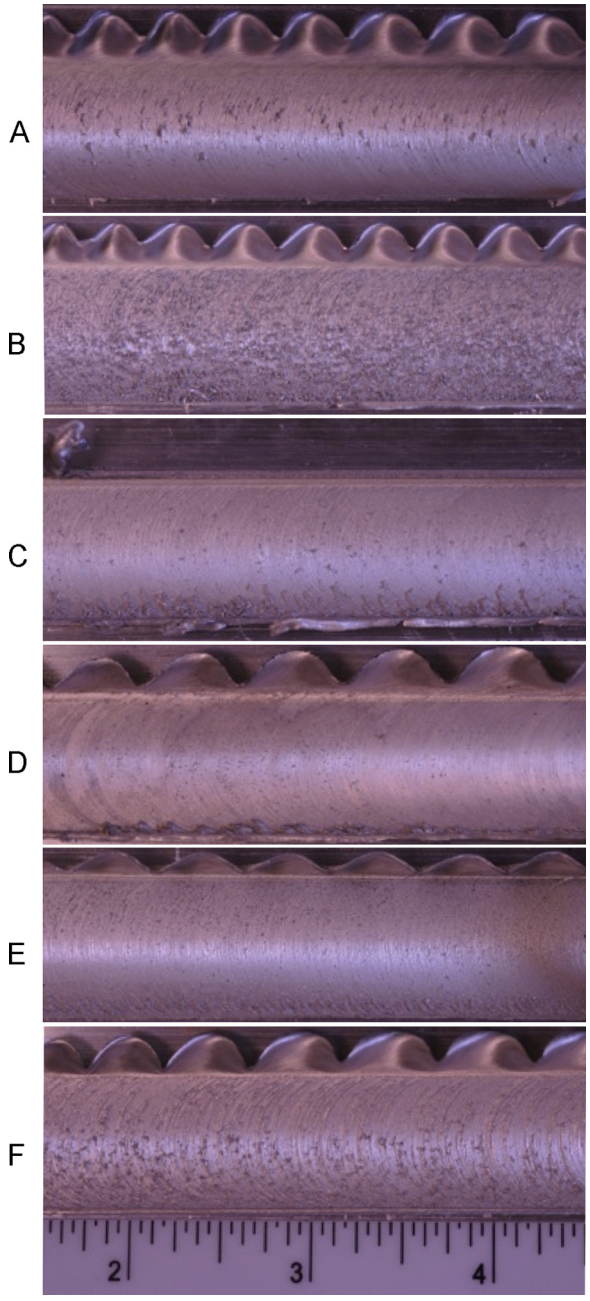

Fig. 6. Top surfaces of experimental welds. Note the degree of galling and flash present. Samples C and E appear to have the best surface finish. Sample C has minimal flash.

all of the welds displayed some degree of galling along the crowns. The weld with the best surface quality – based both on the degree of flash formation and galling – was weld C.

3.2. X-ray radiography

Radiographic inspection of the welds revealed that five of the six welds exhibited incomplete root penetration as shown in Fig. 7. Only weld C appeared to be a complete weld. Sample A displayed the greatest degree of lack of root penetration. Other features visible in the radiographs included the flash formation on the retreating side and galling on the top surfaces of weld F. Light spots on some of the radiographs appear to indicate either embedded foreign material or material deposited on the tops of the welds. Examples of these spots can be observed in the radiograph of weld C.

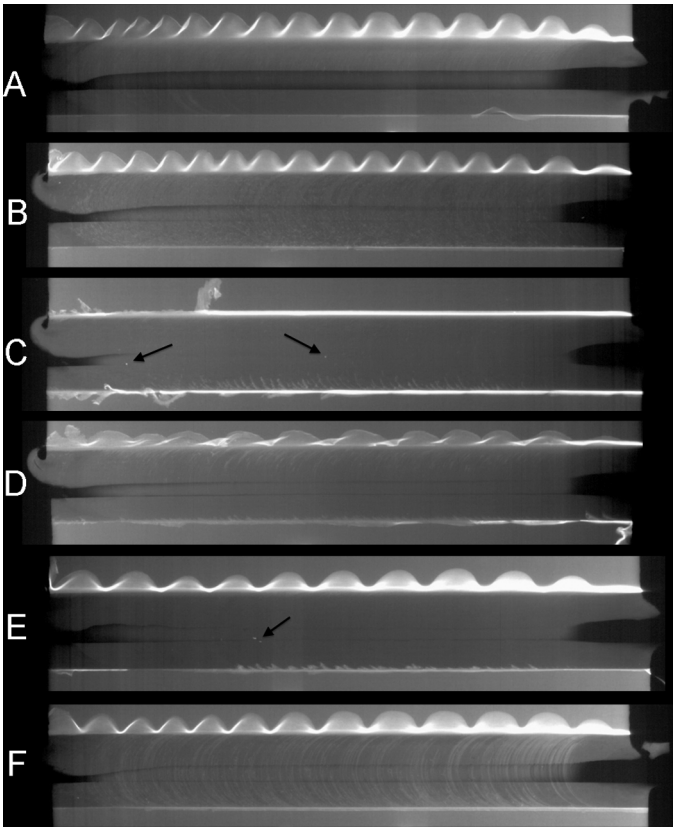

Fig. 7. X-ray radiographs of the six welds produced in this study. Dark lines along the nugget regions of the welds indicate insufficient root penetration that was not visible during the visual inspection. Only weld C appears to be complete. Galling, indicated by light, semi-circular patterns, is visible in welds B and C. White spots (indicated by arrows), which may be indicators of tool wear debris, are also visible in welds C and E.

3.3. Scanning electron microscopy/energy dispersive spectroscopy

A scanning electron microscopy/energy dispersive spectroscopy (SEM/EDS) examination was conducted on those samples exhibiting excessive galling (welds B and F) and those samples suspected of having tool wear debris within the weld as indicated by radiography (welds C and E). The weld crowns and transverse metallographic specimens were analyzed with EDS to determine if evidence of tool debris could be found in the welds. The major energy peaks in each of the spectra were for aluminum with minor peaks for magnesium, silicon, and oxygen. The spectra were consistent with analysis of a 6000 series aluminum alloy. The presence of titanium or iron – the major elements of the tooling – was not detected in any of the EDS spectra.

3.4. Tensile testing

The mean properties obtained from the weld sample tensile tests are summarized in Table 1. As expected, the weld strengths obtained were lower than those of standard aluminum 6061-T6. Weld C exhibited the greatest strength and had a ductility that was equal to the mean of the study samples.

The location of the fracture for each of the weld samples is also indicated in Table 1. Except for weld E, the fracture locations varied between the advancing and retreating portions of the welds; only sample E broke within the weld nugget region, below the void associated with the lack of root penetration.

Table 1
Mean weld mechanical properties and fracture locations.

Sample	Yield strength (MPa) (0.2% offset method)	Tensile strength (MPa)	Elongation (%)	Fracture location
A	124.2	173.1	5.5	Adv./Adv.
B	124.8	192.4	8.0	Adv./Adv.
C	137.1	209.3	7.5	Adv./Retr.
D	133.8	204.5	8.5	Adv./Adv.
E	124.3	197.2	6.5	Nugget/Nugget
F	126.8	191.5	9.0	Retr./Retr.
6061-T6 (typical)[a]	276	310	12[b]	

[a] ASM International (1990).
[b] 1.6 mm thick sample.

3.5. Metallography

Etched short transverse macrograph sections obtained from each weld are shown in Fig. 8. The overall metallurgical structure of the welds is visible in the photos. A range of grain sizes was observed in the microstructures. The degree of lack of root penetration for each weld is also visible in the figure. Only weld C appears complete while weld A shows the greatest degree of void formation.

Weld line remnants (see Fig. 9), commonly called the "Lazy S" defect, were also visible in each of the welds extending from the retreating side, passing through the weld center, and up the advancing side.

3.6. Microhardness measurements

Microhardness profiles obtained from each of the welds are presented in Figs. 10 and 11. Very little variation was observed between the hardness measurements taken along the top, center, and bottom of each weld; therefore, only the center measurements are shown in the figures. The overall shape of the microhardness profile is the characteristic "W" commonly observed in friction stir welds. The hardness profiles for each weld were similar with only minor variation observed in the weld nugget hardnesses and in the widths of the thermomechanically affected zones (TMAZ). The weld region with the greatest hardness was near the base metal with the minimum hardness occurring in the transition between the thermo-mechanically affected and the heat-affected zones (52–55 HV). The weld nuggets all exhibited intermediate hardness (70–80 HV).

4. Discussion

Based on the experimental results, it is concluded that the weld produced with tool C (raised, spiral shoulder features) was the best weld based on surface quality, soundness, and tensile strength. Differences in surface quality, microstructure, and tensile strength are discussed below.

4.1. Surface quality and weld defects

A prominent visual feature present on each of the sample welds in this study is the retreating side flash. This flash was present on all of the welds except weld C. Lohwasser and Chen (2010) report that flash formations of this magnitude are due to high welding temperatures. Clearly, a large degree of metal was displaced by the pin and not contained by the shoulder, resulting in the lack of root penetration visible in the X-ray radiographs. The weld parameters selected for this experiment (the combination of rotational and weld speeds and plunge depth) appear to have heated the metal to high temperatures, providing ease of metal flow, and making it difficult for the tooling to constrain the displaced metal. The straight pins (as opposed to tapered pins) used in the tool design may have further exacerbated the operational conditions

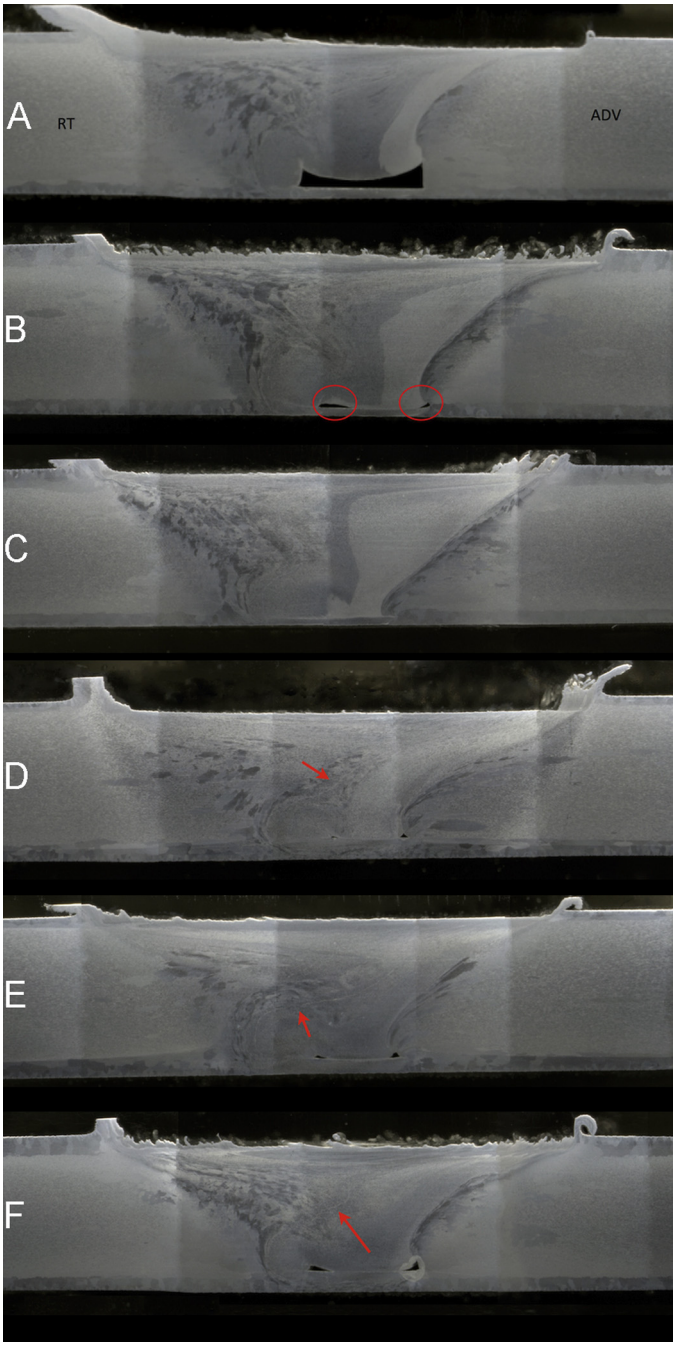

Fig. 8. Short transverse macrographs of welds produced in this experiment. Visible in all of the welds except "C" are voids near the weld roots, indicating incomplete welds. Flash is also visible adjacent to the weld crown in each of the welds. Arrows indicate the presence of joint line remnants (Lazy S defect).

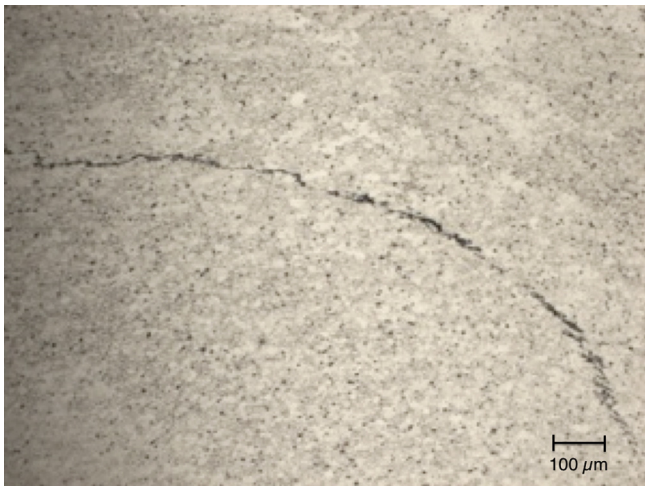

Fig. 9. Weld-line remnant present in sample D (location indicated by arrow in Fig. 8).

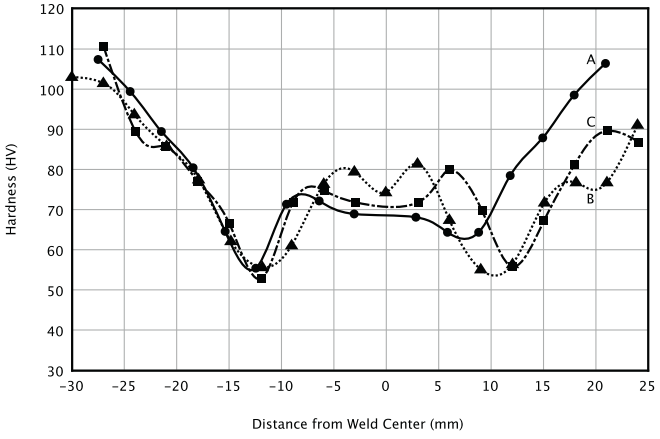

Fig. 10. Vickers hardness (500 g load) measurements taken from short-transverse sections of weld samples A, B, and C.

leading to void formation. A further compounding factor may have been the rough surfaces associated with the rapid-manufactured Ti–6Al–4V shoulders. Because this is a layered-manufacturing technique, small grooves form between layers of material, which may have increased the kinetic coefficient of friction with the aluminum (compared to steel tooling) and thereby increased the frictional heating. Accumulation of weld metal in the grooves and pockets of the shoulders likely contributed to the galling observed on all of the weld crowns. Given the demanding welding parameters, only tool C was able to provide sufficient weld metal containment to produce a sound weld.

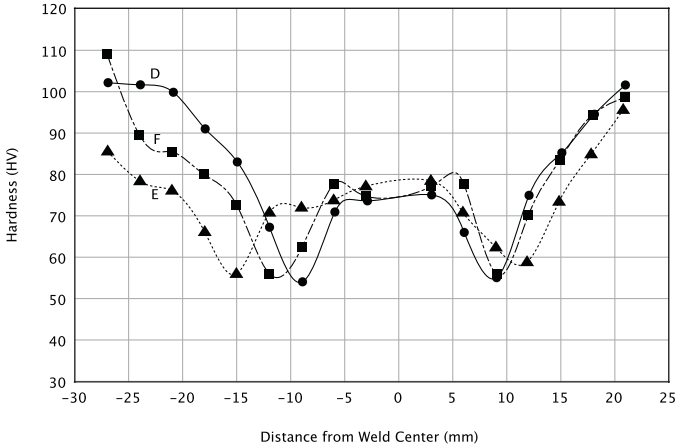

Fig. 11. Vickers hardness (500 g load) measurements taken from short-transverse sections of weld samples D, E, and F.

In order to test the effect of a wiper feature (a flat surface along the outer shoulder edge) on the surface finish of friction stir welds, tools A and B were designed with similar features, except that tool A included a wiper. The purpose of the wiper is to smooth the metal after the weld in order to improve the weld surface finish. A comparison of the surface finish of the welds produced with these two tools reveals that the surface finish of weld A was better than that of weld B, confirming that the inclusion of a wiper improves weld surface finish.

Inspection of the weld radiographs revealed small areas of dense material present either on or in the welds. These areas appear as white spots (Fig. 7) on the radiographs. The most likely explanation for these spots is thought to be tool debris left along the weld. However, the EDS analysis did not provide evidence of the presence of titanium or iron along the weld crown or in the transverse sections. In addition, no metallographic evidence of debris was observed in the short transverse samples. Given the limited sampling provided by the short transverse specimens, the presence of tool debris cannot be completely ruled out, but evidence of major tool wear and debris in the welds was not found.

As stated in the experimental results, weld line remnants (Lazy S defects) were observed in each of the welds. Lazy S defects are caused by the entrapment of oxides from the faying surfaces that did not break up to a significant degree during the welding process. Surface preparation in this study consisted of cleaning the faying surfaces with isopropyl alcohol. In order to eliminate the Lazy S defect, it may be necessary to more thoroughly prepare the faying surfaces (e.g. mill surfaces) or to use a pin with a scroll feature to ensure surface oxides are more completely sheared.

4.2. Microstructure and microhardness

The overall weld structures in this study were typical of those observed in friction stir welds. A central weld nugget was present surrounded on each side by a thermomechanically affected zone (TMAZ). The minimum weld hardness occurred at the edge of the TMAZ, leading into the adjacent heat-affected zone (HAZ). As expected, the hardness increased through the HAZ leading into the base metal. One feature that was not observed in these welds is the common onion ring structure typically observed in friction stir welds. Onion ring structures are thought to occur as layers of metal shear and flow during the weld process, producing layers of fine-grained, dynamically recrystallized metal. Instead, the welds in this study displayed a wide range of grain sizes with some regions of fine-grained structure interspersed within regions of course-grained metal. Lohwasser and Chen (2010) have shown that weld structures similar to these are due to weld nugget collapse, a characteristic associated with hot weld conditions. Attempts to measure the grain size within different regions of the welds were unsuccessful because uniform etching to reveal grain structure proved extremely difficult given the wide range of grain size.

4.3. Tensile properties and fracture location

Weld C exhibited the greatest yield and tensile strength of the welds in this study. The presence of defects, especially the lack of root penetration, has the effect of decreasing the weld tensile strength. The tensile strength of the experimental welds is inversely related to the size of the void associated with lack of root penetration for each weld – with the lowest strength associated with weld

A (largest void) and the highest strength associated with weld C (no discernable void).

The fracture location of tensile test samples may give clues about the quality of the weld and particularly the presence of defects. Tensile test samples of mechanically sound friction stir welds are expected to fracture in the transition between the thermomechanically affected zone and heat affected zone, where the hardness is lowest. The presence of weld defects in the weld nugget may lead to fracture within that region. In most of the welds, differences in the minimum hardness between the advancing and retreating side were insignificant. Therefore, the welds in this study fracture on both the retreating and advancing sides with no clear pattern discernable. Only weld D fractured in the central nugget region. This was surprising because there was no radiographic or metallographic evidence for large voids in this region of the weld, especially compared to weld A. Microhardness measurements also did not indicate unusually low hardness in the central nugget region. It is thought that the particularly severe Lazy S defect (see Fig. 9) may have contributed to the fracture in the weld nugget region of this weld.

5. Conclusions

Based on the results of this experiment it can be concluded that:

- Shoulder features in the form of a raised spiral (tool C) have the greatest potential for producing high quality welds even under non-ideal process conditions.
- Shoulder wipers improve the surface finish of friction stir welds.
- Additive manufacturing shows promise as a route to producing FSW tools with unique shoulder and pin features that would otherwise be difficult to machine.

Acknowledgements

The authors gratefully acknowledge the financial support of this research provided by the Material and Processes Branch at NASA Johnson Space Center.

References

. ASM Handbook, vol. 2., tenth ed. ASM International, Materials Park, OH.
Elangovan, K., Balasubramanian, V., 2008. Influences of tool pin profile and tool shoulder diameter on the formation of friction stir processing zone in AA6061 aluminium alloy. Mater. Des. 29, 362–373.
Lohwasser, D., Chen, Z., 2010. Friction Stir Welding: From Basics to Applications. Woodhead Pub., Cambridge, pp. 15–41, 83–212, 245–276.
Mandal, N.R., 2002. Aluminum Welding. Narosa Pub. House, New Delhi, India, pp. 149–166.
Mishra, R.S., Mahoney, M.W., 2007. Friction Stir Welding and Processing. ASM International, Materials Park, OH, pp. 1–5, 7–28, 51–55.
Rafi, H.K., Karthik, N.V., Gong, H., Starr, T.L., Stucker, B.E., 2013. Microstructures and mechanical properties of Ti6Al4V parts fabricated by selective laser melting and electron beam melting. J. Mater. Eng. Perform. 22, 3872–3883.
Scialpi, A., De Filippis, L.A.C., Cavaliere, P., 2007. Influence of shoulder geometry on microstructure and mechanical properties of friction stir welded 6082 aluminium alloy. Mater. Des. 28, 1124–1129.